# 6. Arthritis and Cartilage

**BOOK CHAPTER**

# Arthritis and Cartilage

Nancy M. Major MD (chapter://search/Major%20Nancy M./%7B%22type%22:%22author%22%7D), Mark W. Anderson MD (chapter://search/Anderson%20Mark W./%7B%22type%22:%22author%22%7D), Clyde A. Helms MD (chapter://search/Helms%20Clyde A./%7B%22type%22:%22author%22%7D), Phoebe A. Kaplan MD (chapter://search/Kaplan%20Phoebe A./%7B%22type%22:%22author%22%7D) and Robert Dussault MD (chapter://search/Dussault%20Robert/%7B%22type%22:%22author%22%7D)
Musculoskeletal MRI (chapter://browse/book/3-s2.0-C20130189064), 6, 118-131

## How to Image Arthritis and Cartilage

**Magnetic resonance imaging ( MRI )** remains the ideal imaging technique for evaluating articular cartilage, as it allows for direct visualization of the cartilage and subchondral bone, and its multiplanar capability and exquisite soft tissue contrast provide unparalleled information about structures in and around the joint space. Although the diagnosis of the type of arthritis is made with conventional radiographs, evaluation with MRI can demonstrate changes in the articular cartilage, assess for loose bodies within the joint space, and determine synovial involvement, thereby aiding in treatment planning.

- *Coils and patient position:* The joint being imaged determines which coil and which position are used. In the knee, the

standard extremity coil is used in the same manner as imaging for a torn meniscus. The same would hold for the wrist, elbow, and so forth.

• *Image orientation:* Joints imaged for arthritis and for cartilage are best seen with the standard planes of imaging discussed in other chapters. In the knee, three planes (axial, coronal, and sagittal) should be used to evaluate the cartilage adequately.

• *Pulse sequences and regions of interest:* For imaging a joint for arthritis, it is recommended that T1-weighted (T1W) and some type of T2-weighted (T2W) sequence be used in each plane of imaging. Cartilage-sensitive sequences are discussed in greater detail later in this chapter.

• *Contrast:* Contrast is often utilized for the diagnosis of synovial involvement, as well as assessing for treatment response because it markedly increases the conspicuity of hypertrophied synovium (pannus).

Most joint abnormalities are discussed in the chapters addressing specific joints (e.g., avascular necrosis in the marrow or hip chapters). This short chapter discusses a few additional abnormalities that can affect any joint, such as pigmented villonodular synovitis (PVNS), synovial chondromatosis, and a few common arthritides; it also provides an overview of cartilage imaging.

Current trends in rheumatology suggest that MRI is a valuable tool for assessing synovitis and allowing for aggressive and earlier treatment. Awareness of findings associated with the arthropathies

is important, as the changes encountered can be seen in patients undergoing imaging for other reasons.

## Rheumatoid Arthritis

Early diagnosis and treatment have been recognized as essential for improving clinical outcomes in patients with rheumatoid arthritis (RA). The erosive changes in RA can be detected earlier with MRI than conventional radiographs, allowing for earlier diagnosis and treatment ( Fig. 6.1 (f0010) ). It has been recognized that bone marrow edema, a precursor to the development of erosions, can be readily seen on MRI and may be a sign of active inflammation. The location of the bone marrow edema is important, because inflammation at tendon and/or ligamentous insertions may signify a peripheral spondyloarthropathy rather than RA.

**Fig. 6.1**

**Rheumatoid arthritis. A** , Coronal T1W image in a patient with advanced rheumatoid arthritis reveals multiple erosions throughout the metacarpophalangeal joints and wrist. **B** , Coronal fat-suppressed T1W image after intravenous gadolinium administration highlights the associated enhancing synovial pannus in these regions.


Careful evaluation of T1W images of a joint affected by RA may reveal slightly higher signal intensity within pannus relative to joint fluid, allowing for identification without the need for intravenous contrast administration. In many cases, however, pannus cannot be reliably differentiated from synovium and joint fluid using standard imaging sequences ( Fig. 6.2 (f0015) ). After the intravenous administration of gadolinium, the hypervascular pannus can be easily identified because of its intense enhancement. It has also been reported that contrast-enhanced T1W images identify more periarticular bone abnormalities than fat-suppressed T2W images. Previously, treatment of RA was not predicated on the amount of

pannus present, but rheumatologists have become more aggressive in initiating treatment, and MRI is often done to evaluate pannus and help in the design of a treatment plan.

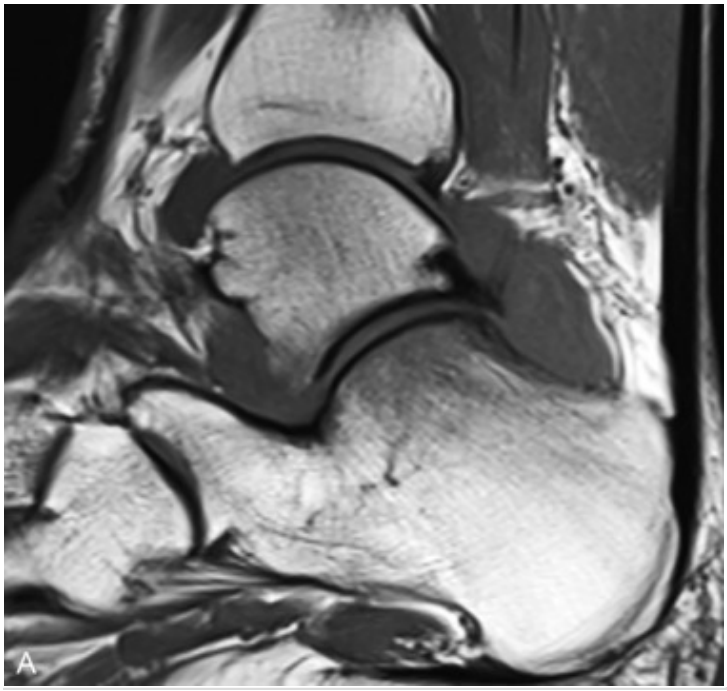


**Fig. 6.2**

**Rheumatoid arthritis. A** , **B** , and **C** , Sagittal T1W, fat-saturated T2W and postgadolinium fat-saturated T1W images demonstrate extensive pannus throughout the subtalar and tibiotalar joints. Note the difference between enhancing pannus ( *arrows* ) and nonenhancing joint fluid ( *arrowhead* ) in **C** .

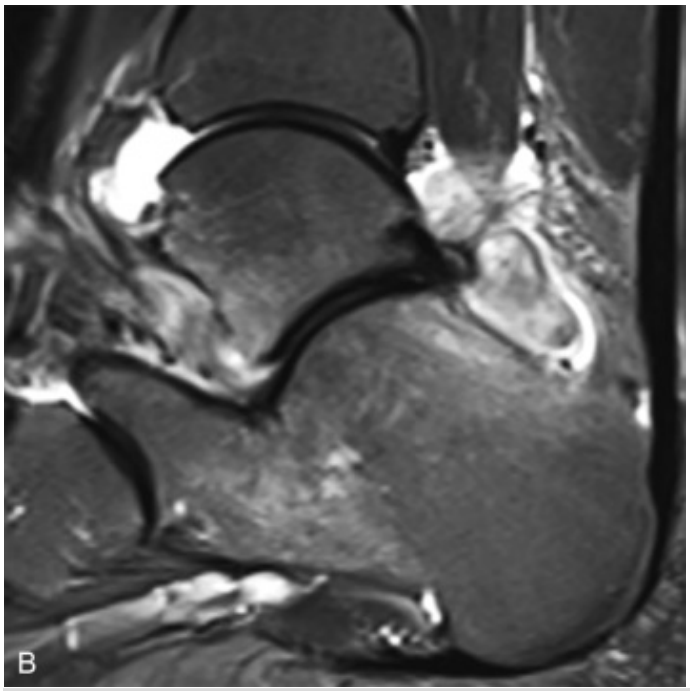

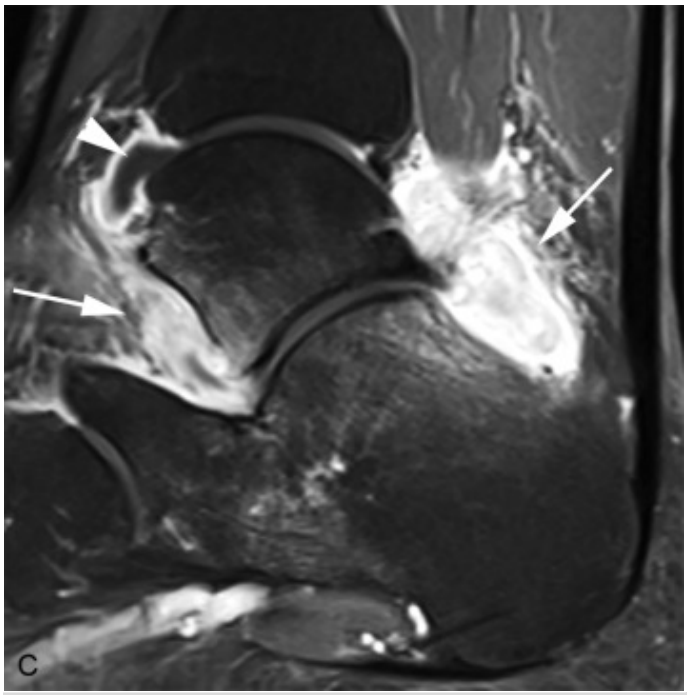


Occasionally, a swollen joint in a patient with RA will contain multiple small, loose bodies, called *rice bodies* ( Fig. 6.3 (f0020) ). These occur in certain chronic synovial conditions such as RA or indolent infections when the synovial villi hypertrophy to such an extent that they outgrow their blood supply, necrose, and slough off into the joint. They are called *rice bodies* because of their resemblance at surgery to white rice. On MRI, rice bodies can mimic multiple loose bodies or synovial chondromatosis, but typically rice bodies are much smaller than the bodies of synovial chondromatosis and remain low signal on T2W images. Most, but not all, patients already carry a diagnosis of RA, so the entity is easily recognized as rice bodies if the radiologist is familiar with this process. Rice bodies can be removed easily by a surgeon if they cause mechanical symptoms, but otherwise the treatment is the same as for any joint involved with RA.

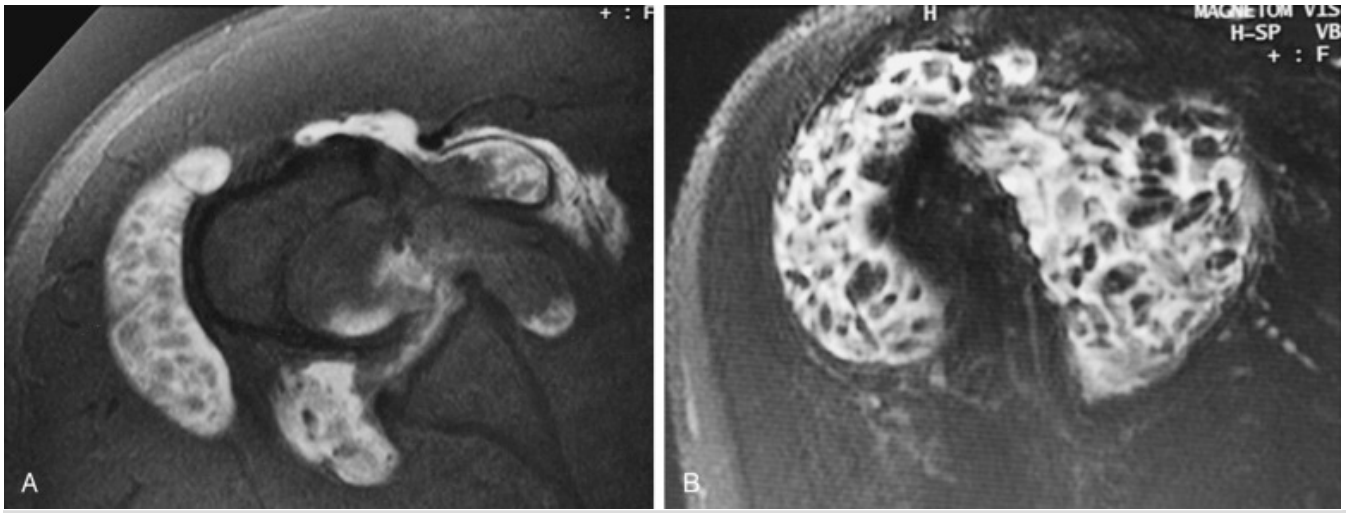


**Fig. 6.3**

**Rheumatoid arthritis.** **A** and **B** , T1W images with fat suppression after a gadolinium arthrogram in the axial ( **A** ) and oblique ( **B** ) coronal planes through the shoulder show multiple small filling defects or loose bodies. At surgery, these were found to be rice bodies.

## Ankylosing Spondylitis

Generally, the changes of ankylosing spondylitis can be appreciated with conventional x-ray. The early changes such as enthesopathy producing inflammation and marrow edema at tendon or ligament insertion sites can be appreciated much earlier on MRI than with conventional x-ray and as such, MRI is useful in the early diagnosis of the disease. In addition to the enthesopathic changes, the presence of bone marrow edema at the sacroiliac joints as well as the vertebral body corners (“shiny corners”) will aid in early diagnosis and treatment and are evident earlier on MRI than on x-ray ( Fig. 6.4 (f0025) ). The administration of intravenous contrast to assess the degree of enhancement may also assist with treatment planning.

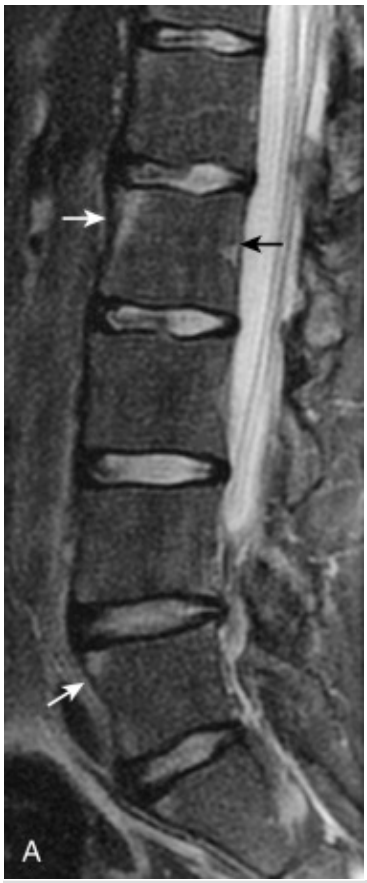


**Fig. 6.4**

**Ankylosing spondylitis. A** , Sagittal fat-suppressed T2W image shows increased signal at anterior superior aspects of L2 and L5 ( *white arrows* ). Note the loss of the normal concave posterior margin of the vertebral body ( *black arrow* ). **B** , Coronal fat-suppressed T2W image shows bone marrow edema on both sides of the sacroiliac joints in this patient with ankylosing spondylitis.

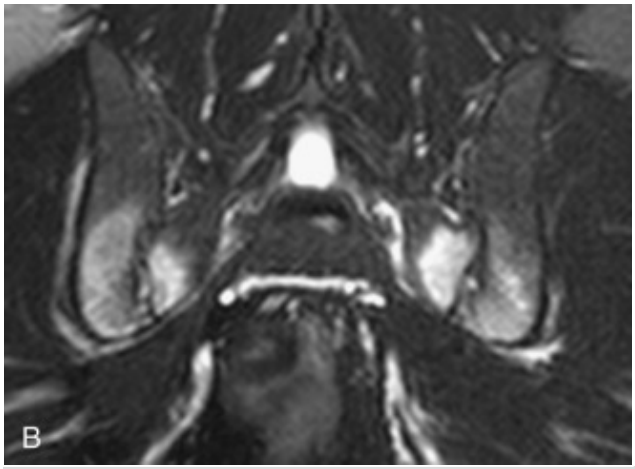


## Gout

As with RA, the radiographic findings in gout are typically sufficient for diagnosis, and MRI has little to offer in this disease. It is important to appreciate, however, that gouty tophi occasionally are seen in patients not known to have gout, in which case they can cause diagnostic confusion. Gouty tophi can occur in almost any soft tissue location and may erode bones or begin within a bone (intraosseous tophus). In cases in which the tophus is large and the diagnosis of gout is unknown, the tophus can be misdiagnosed as a tumor with resultant biopsy. Tophi are typically low in signal on T1W and T2W images ( Fig. 6.5 (f0030) ), which distinguishes them from most other types of joint pathology and from most tumors (with the exception of fibrous tumors, PVNS, and amyloid). Tophi occasionally demonstrate increased signal intensity on MR images ( Fig. 6.6 (f0035) ) and may show uniform contrast enhancement or have a nonenhancing center. MRI can also reveal cortical erosion related to an adjacent tophus due to the associated bone marrow edema.

**Fig. 6.5**

**Gout. A,** Anteroposterior radiograph of the knee shows faint radiodensities along the medial and lateral aspects of the joint compatible with tophi, as well as associated osseous erosions ( *arrowheads* ). **B** and **C** , Coronal and axial fat-saturated T2W images demonstrate heterogeneous, predominantly low signal intensity tissue in these regions ( *arrows* ), as well as one of the erosions ( *arrowhead* ).


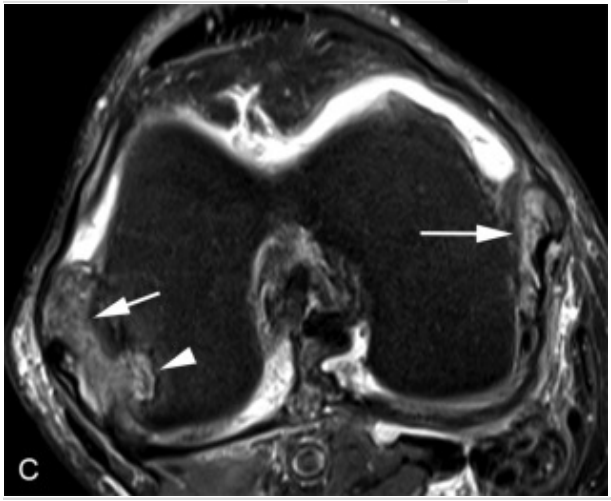


**Fig. 6.6**

**Gout. A** , Anteroposterior radiograph of the foot demonstrates a dense soft tissue tophus and associated erosion along the medial margin of the first metatarsal head. **B** , **C** , and **D** , Long-axis T1W, fat-saturated T2W, and postgadolinium fat-saturated T1W images show similar findings. Note the low signal intensity of the tophus in **B** as well as its relatively diffuse enhancement in **C** .

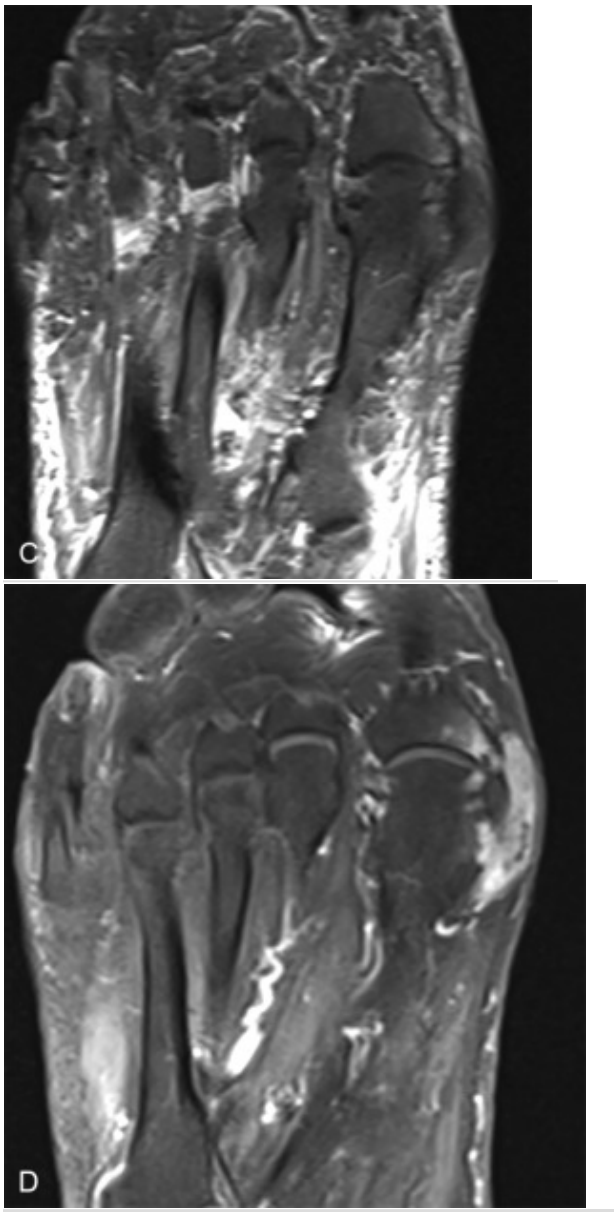


Because of the nonspecific features of gout on MRI, supporting features include the site of involvement and distribution of the findings. The lack of an overlying or contiguous ulcer can distinguish gout in the foot from osteomyelitis. The popliteus and patellar tendons in the knee have a predilection for gout involvement ( Fig. 6.7 (f0040) ). Clinically, the patient may present with a mass. If not familiar with the appearance and location, this finding may be misconstrued as a soft tissue malignancy.


**Fig. 6.7**

**Gout.** Sagittal proton density ( **A** ) and STIR ( **B** ) images reveal lobular, masslike tissue within the distal patellar tendon demonstrating mixed but predominantly low signal intensity on both images ( *arrowheads* ). Biopsy revealed gout.


## Calcium Pyrophosphate Dihydrate Deposition

MRI has little to offer in the diagnosis of calcium pyrophosphate dihydrate deposition (CPPD), or pseudogout. The appearance of chondrocalcinosis in the menisci of the knee has been reported to have linear high signal that can mimic a meniscal tear, but this has not been a significant pitfall in our experience. One might

intuitively think that calcification would produce low signal on MR images; however, in some cases, calcification paradoxically causes intermediate to high signal on T1W images. The reason for this has not been determined, but several theories have been discussed in the literature. Chondrocalcinosis also can appear as linear or punctate areas of low signal in hyaline cartilage, which are particularly noticeable on T2* sequences because of the associated blooming artifact ( Fig. 6.8 (f0045) ). A utility of MRI in the evaluation of CPPD is to assess the degree of cartilage loss associated with the arthropathy, which can be more accurately assessed with MRI than with radiographs so that appropriate treatment planning can be instituted in a timelier fashion.


**Fig. 6.8**

**CPPD/chondrocalcinosis. A** , Anteroposterior radiograph of the knee shows extensive chondrocalcinosis. **B** , Coronal gradient echo image demonstrates prominent low signal intensity foci (“blooming” effect) at sites of calcium deposition within the articular cartilage ( *arrowheads* ).


## Hemophilia

Although patients with hemophilia are not often imaged with MRI, some of the findings seen in hemophilia are worth mentioning. The associated arthropathy and joint destruction are often well assessed with conventional radiographs. Repetitive hemarthroses leave deposits of hemosiderin, however, which is seen on MR images as clumps of low signal lining the synovium on T1W and T2W images ( Fig. 6.9 (f0050) ). This has been termed *hemosiderotic arthropathy* . The amount of hemosiderin varies from none to moderate but is almost never as prominent as that seen in PVNS. In joints with extensive hemosiderin, there is typically advanced joint destruction, which is uncommon in PVNS, but it is virtually never a diagnostic dilemma to differentiate hemophilia from PVNS because patients with hemophilia are well aware of their diagnosis long before a joint is imaged. The main indications for imaging a hemophiliac

joint are to determine the extent of cartilage destruction and the thickness of the synovium, features that help determine how to manage the joint abnormality.

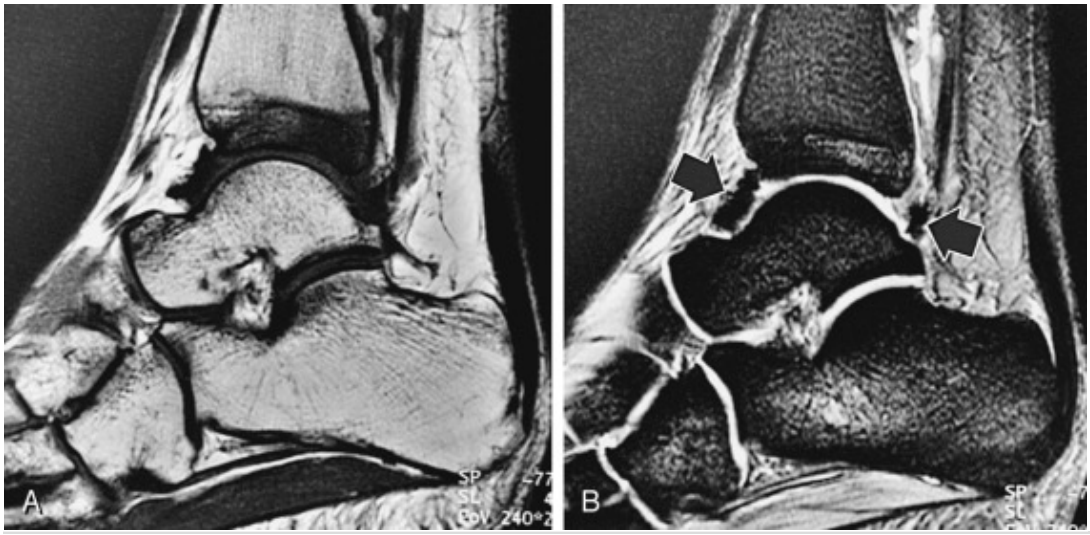


**Fig. 6.9**

**Hemophilia.** **A** and **B** , Sagittal T1W ( **A** ) and gradient echo ( **B** ) images in the ankle of a patient with hemophilia show a large joint effusion that is low in signal on the T2* sequence ( *arrows* ), consistent with hemosiderin deposition.

## Amyloid

Amyloid deposits, often a consequence of dialysis treatment, tend to occur in and around large joints and can cause significant joint swelling and pain ( Fig. 6.10 (f0055) ). Bone erosion can be prominent. Amyloid more commonly affects the spine, where the deposits may be either amyloid or an amyloid-like entity called $\beta_2$-*microglobulin* . Since amyloid or $\beta_2$-microglobulin deposits from renal disease can perfectly mimic infection on radiographs and MR images ( Fig. 6.11 (f0060) ), it is imperative to inquire whether a

patient who displays these MR findings has renal failure or is on dialysis in an attempt to arrive at the correct diagnosis, although in some cases, biopsy may be necessary for definitive diagnosis.

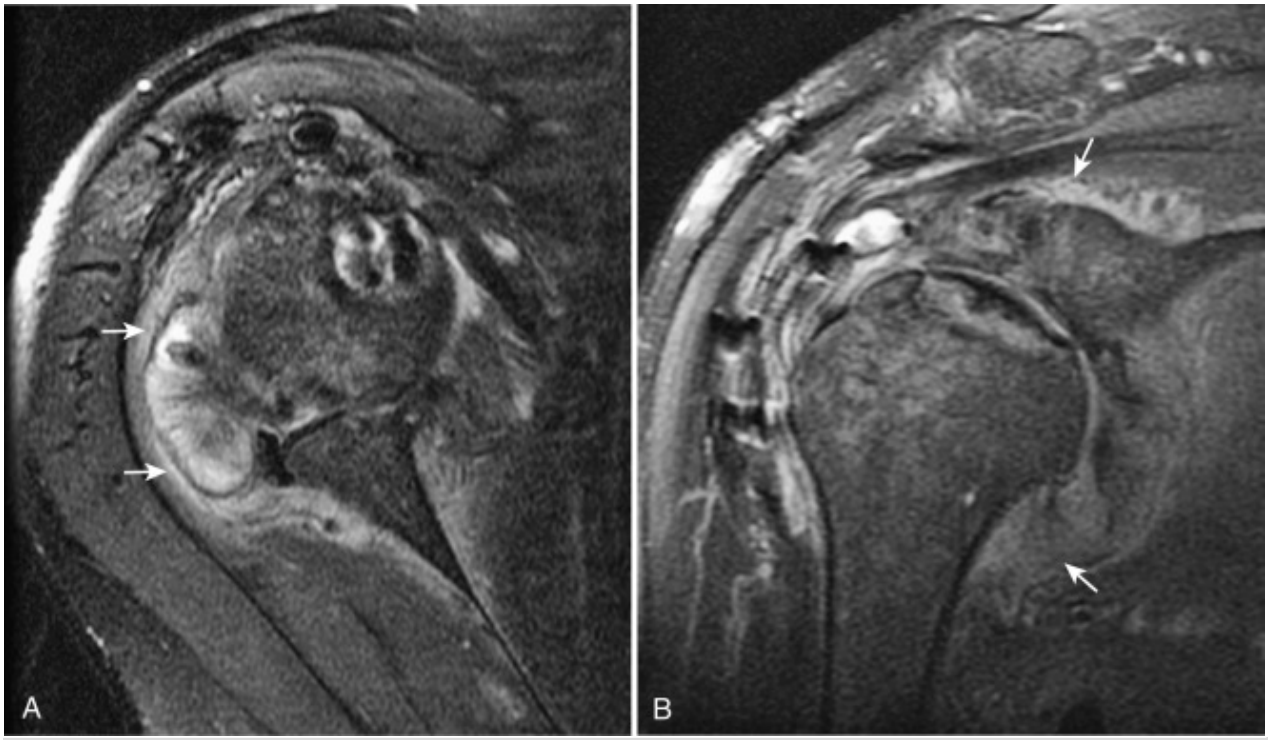


**Fig. 6.10**

**Amyloid. A** , Axial T2W image with fat suppression in a patient with renal failure and prior rotator cuff surgery. Note the low and intermediate signal within the joint space ( *arrows* ). **B** , Coronal T2W image with fat suppression in the same patient as in **A** also shows the low and intermediate signal of amyloid within the joint space ( *arrows* ).


**Fig. 6.11**

**Amyloid. A** , Sagittal T1W image in a patient with back pain and renal failure. End plate irregularity is noted with abnormal disk space. **B** , T2W image with fat suppression shows abnormal signal within the disk space. This process occasionally can be confused with diskitis because of the increased signal in the disk space.

Amyloid deposits often demonstrate low signal intensity on T1W and T2W images, although most examples we have seen in the spine have shown high signal on T2W images. After contrast administration there is typically mild peripheral enhancement. The presence of abnormal soft tissue in the paraspinal or epidural spaces is more suggestive of diskitis rather than amyloid.

## Tumors

There are no tumors that originate in joints, but there are a few entities that are tumor-like and may manifest as a swollen joint. The most common of these are synovial chondromatosis and PVNS

(discussed further). Uncommon entities that can manifest similarly are synovial hemangioma and lipoma arborescens; these are rare enough that they are not discussed further.

## Synovial Chondromatosis

There are two forms of synovial chondromatosis: primary and secondary. Primary synovial chondromatosis is an uncommon entity that is caused by metaplasia of the synovium, which produces multiple loose bodies within a joint. Initially, these are cartilaginous bodies that are not calcified; they generally progress to calcified loose bodies, which are typically of the same size. They may cause mechanical symptoms, as with any loose body in a joint, or they may merely cause a sense of swelling or fullness in the joint. Three phases of primary synovial chondromatosis have been described, and the MRI findings correspond to the different phases. In the first phase, the metaplastic process of the synovium leads to the formation and proliferation of the hyaline cartilaginous bodies without loose intra-articular bodies. When imaged with MRI, this appearance shows a confluent mass of tissue that has the same signal intensity as hyaline articular cartilage. This appearance can be concerning for a tumor/mass, but recalling that no tumors arise within the joint space and the signal intensity is that of hyaline articular cartilage, the diagnosis of primary synovial chondromatosis (in the active stage) can be made, thus avoiding an unnecessary biopsy and an erroneous pathologic diagnosis. The second phase is a combination of synovial cartilaginous proliferation and shedding of intra-articular loose bodies. The third phase is the complete shedding of numerous intra-articular bodies and no active synovial proliferation ( Figs. 6.12 (f0065) and 6.13

(f0070) ). Cartilage erosion from these bodies is a late finding, if it occurs at all. Treatment is removal of the loose bodies and a synovectomy. MRI plays a role in the diagnosis because similar to conventional radiographs, primary synovial chondromatosis resembles PVNS. Although these may be indistinguishable on MRI, low signal intensity masses on all pulse sequences are typical for PVNS, as opposed to intermediate signal bodies demonstrating the same signal intensity as cartilage in primary synovial chondromatosis.


**Fig. 6.12**

**Primary synovial chondromatosis.** **A** and **B** , Anteroposterior radiograph ( **A** ) and axial computed tomography (CT) image ( **B** ) of the hip show innumerable rounded calcifications of relatively uniform size throughout the joint. **C** and **D** , coronal and axial T2W fat-suppressed images of the same patient also show the low signal intensity foci distributed throughout the joint.


B

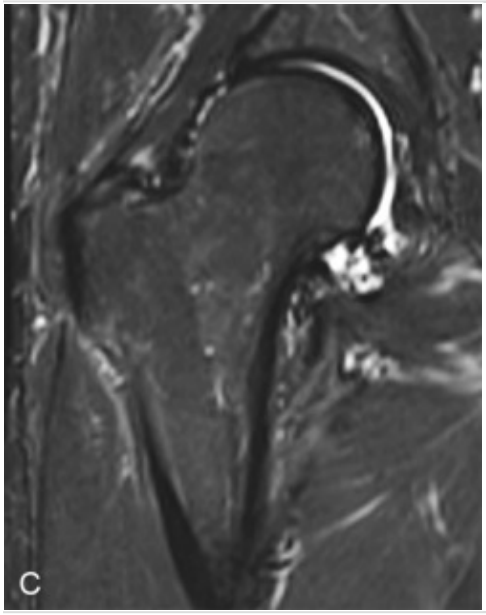
C

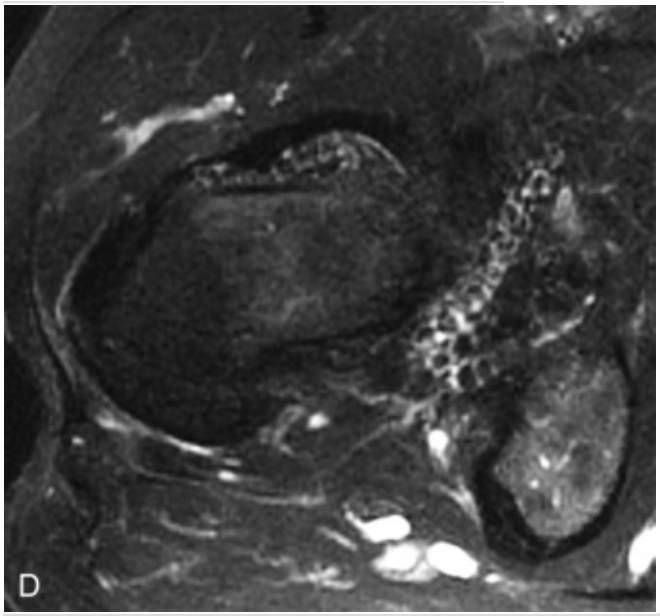
D

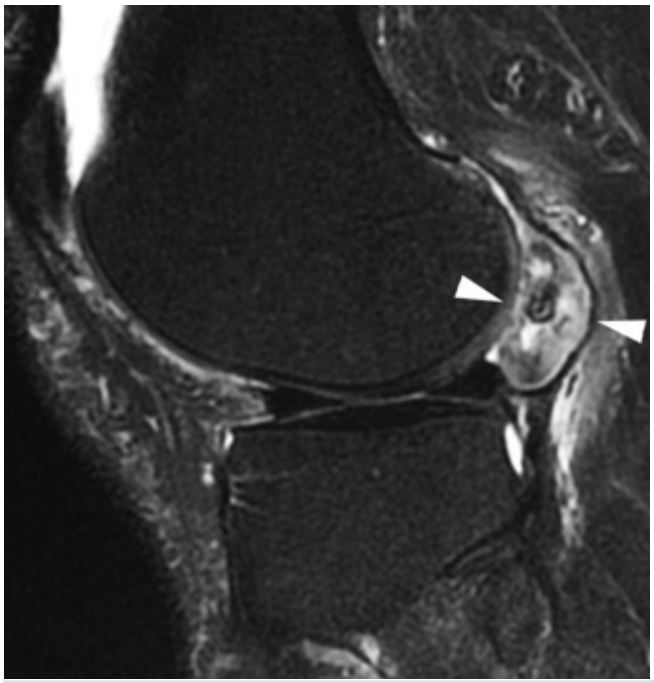

**Fig. 6.13**

**Synovial chondromatosis, focal.** Sagittal STIR image demonstrates a lobular mass in the posterolateral aspect of the knee demonstrating heterogeneous signal intensity ( *arrowheads* ) with a low signal intensity focus centrally. This is a nonspecific appearance, but was resected and shown to be a focus of synovial chondromatosis.

Secondary synovial chondromatosis is a much more common disorder. It is believed to be secondary to trauma, which causes shedding of bits of articular cartilage, resulting in loose bodies in the joint. Secondary synovial chondromatosis is typically an easy radiographic diagnosis, with the presence of multiple calcified loose bodies being virtually pathognomonic. These bodies may or may not calcify and, in contrast to primary synovial chondromatosis, are of different sizes and generally fewer in number ( Fig. 6.14 (f0075) ). Osteoarthrosis is typically present because of the cartilage damage. Treatment is removal of the loose bodies and treatment of any articular cartilage defects. A synovectomy is unnecessary because this condition is not caused by metaplasia of the synovium.


**Fig. 6.14**

**Pigmented villonodular synovitis.** Sagittal proton density ( **A** ) and STIR ( **B** ) images reveal extensive frondlike areas of low signal intensity tissue throughout the knee joint. **C,** Sagittal gradient echo image shows prominent “blooming” of this tissue related to its hemosiderin content. Note also the increased conspicuity of additional synovial involvement in the suprapatellar region ( *arrowheads* ).


## Pigmented Villonodular Synovitis

PVNS is a disorder of unknown cause that can affect any joint, bursa, or tendon sheath (when it affects a tendon sheath, it is called *giant cell tumor of tendon sheath* ). PVNS results in synovial hypertrophy with diffuse hemosiderin deposits within the joint. It virtually never calcifies and causes joint space narrowing only late in its course; radiographs simply show a swollen joint, if anything at all. When a large joint is affected, the hemosiderin can produce a dense effusion that may be detected radiographically.

MRI is virtually pathognomonic. A joint effusion with hypertrophied synovium displaying areas of low signal intensity on T2W images is characteristic (see Fig. 6.14 (f0075) ). The process can erode into bone, making large cystic cavities, but is typically confined to the soft tissues within a joint. Due to the magnetic susceptibility properties of hemosiderin, a gradient echo sequence will demonstrate obvious blooming of the hemosiderin and assist with identifying additional smaller foci, if present.

PVNS has two presentations in joints: diffuse and focal. When PVNS is diffuse, it requires a total synovectomy for treatment, which is difficult to perform, and recurrence is common. In focal PVNS (also called *focal nodular PVNS* ), resection is considerably easier and more effective ( Fig. 6.15 (f0080) ). When PVNS is identified within the joint, the remainder of the joint should be carefully inspected to identify other deposits. Because additional foci may change the management of the patient, this inspection may necessitate increasing the field of view, particularly in the knee, to evaluate the entire suprapatellar pouch (see Fig. 6.14 (f0075) ).


**Fig. 6.15**

**Pigmented villonodular synovitis, focal.** **A** and **B** , Sagittal proton density ( **A** ) and STIR ( **B** ) images display an ovoid mass containing foci of low signal intensity. This was shown to be focal (nodular) PVNS on biopsy.


## Loose Bodies

Loose bodies in joints can be difficult to find with any imaging modality, but MRI seems to be better than most techniques. MR arthrography is superior to plain MRI, unless a large joint effusion is present. Loose bodies can be composed of cartilage or bone ( Fig. 6.16 (f0085) ). We try to include a gradient echo sequence in at least one plane when looking for loose bodies in the hope that if they contain any cortical bone, they will “bloom” and be more easily seen. Loose bodies are most often encountered in the knee but can occur in any joint.

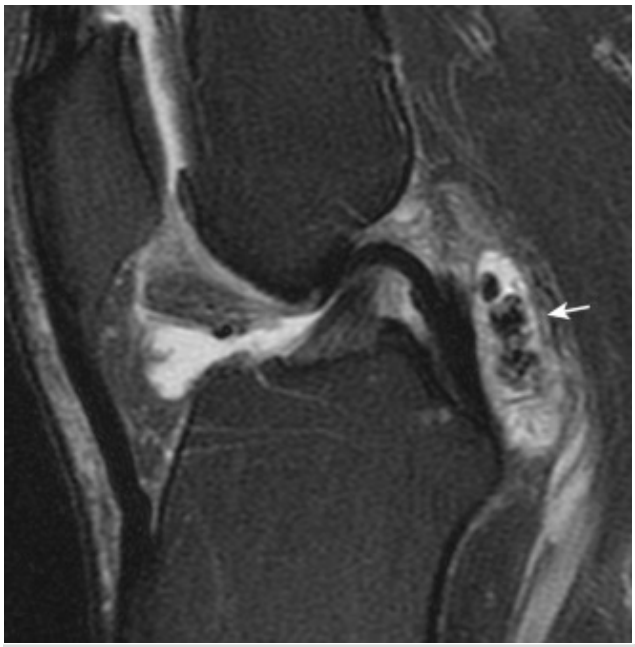

**Fig. 6.16**

**Loose bodies (secondary synovial osteochondromatosis).** Multiple ossified loose bodies of varying size ( *arrow* ) consistent with the diagnosis of secondary synovial chondromatosis.

## Cartilage

Cartilage research continues to be an area of active musculoskeletal investigation. Many articles have been published on MRI of cartilage comparing various imaging sequences for their utility in diagnosing chondral abnormalities. Which sequence is really the best is debatable, but so far no single sequence is indisputably better than all the others. It is imperative that every knee MRI examination have a cartilage-sensitive sequence. Some of the cartilage sequences promulgated in the literature are not readily available on commercial magnets, and others require inordinate imaging times, which renders them useless for routine use. Some of the newer techniques include T2 mapping, delayed gadolinium-enhanced MR imaging of cartilage (dGEMRIC), T1ρ *(rho)* imaging, sodium imaging, and diffusion-weighted imaging. Some authors

recommend specialty sequences be employed only when cartilage abnormalities are suspected, but you had better suspect a cartilage abnormality in every knee and have a sequence that shows the cartilage to good advantage, or your orthopedic surgeon will look elsewhere for imaging services. Cartilage lesions often accompany other pathologies and may be an unsuspected cause of joint pain.

Cartilage treatment has become important in orthopedic surgery.

Multiple grading systems for cartilage abnormalities have been described in the radiology and orthopedic surgery literature. One radiologist's grade 2 lesion is another's grade 3. Simply saying there is a grade 2 or 3 cartilage abnormality leaves one wondering which grading scale is being employed. It can get very confusing and is often misleading. No single grading system seems to have a majority of proponents; we do not recommend a description of the cartilage using a grading system in routine clinical practice. A simple description of the MRI appearance should be adequate for treatment purposes and allows the referring clinician to place the lesion into his or her particular grading system. Clinical research studies utilize semi-quantitative scoring methods such as WORMS ( *w* hole- *or* gan *M* R imaging *s* core), KOSS ( *k* nee *o* steoarthritis *s* coring *s* ystem), and BLOKS ( *B* oston- *L* eeds *o* steoarthritis *k* nee *s* core). These scoring systems assess morphologic characteristics of cartilage in conjunction with other structures around the knee to establish risk factors for pain and progression of disease in patients with knee osteoarthritis. The terms are introduced for you to be aware of surgical considerations, but we will not further elaborate on these scoring techniques.

Descriptions of the cartilage should state whether there is focal abnormal signal, surface fibrillation or irregularity, fissuring ( Fig. 6.17 (f0090) ), a partial-thickness defect ( Fig. 6.18 (f0095) ), or a full-thickness defect ( Fig. 6.19 (f0100) ) and if the underlying bone has abnormal signal ( Figs. 6.20 (f0105) and 6.21 (f0110) ). We refrain from commenting on generalized thinning of the cartilage because it is virtually impossible to document at arthroscopy. Cartilage thickness seems to depend on patient age and activity, is not relevant to any symptoms or therapy that has been described, and probably has a better-than-even chance of being an inaccurate assessment. One particular cartilage abnormality that is important to recognize, however, is that of delamination. This refers to separation of the cartilage from the underlying bone and is diagnosed when fluid signal intensity is identified along the tidemark at the cartilage–bone interface (see Fig. 6.21 (f0110) ). This is an important finding because the majority of the abnormality may not be visible at arthroscopy.

## Fig. 6.17

**Cartilage fissure.** Coronal ( **A** ) and axial ( **B** ) fat-suppressed T2W images demonstrate a deep cartilage fissure along the weight-bearing surface of the medial femoral condyle ( *arrowheads* ), as well as prominent edema-like signal intensity in the underlying bone.

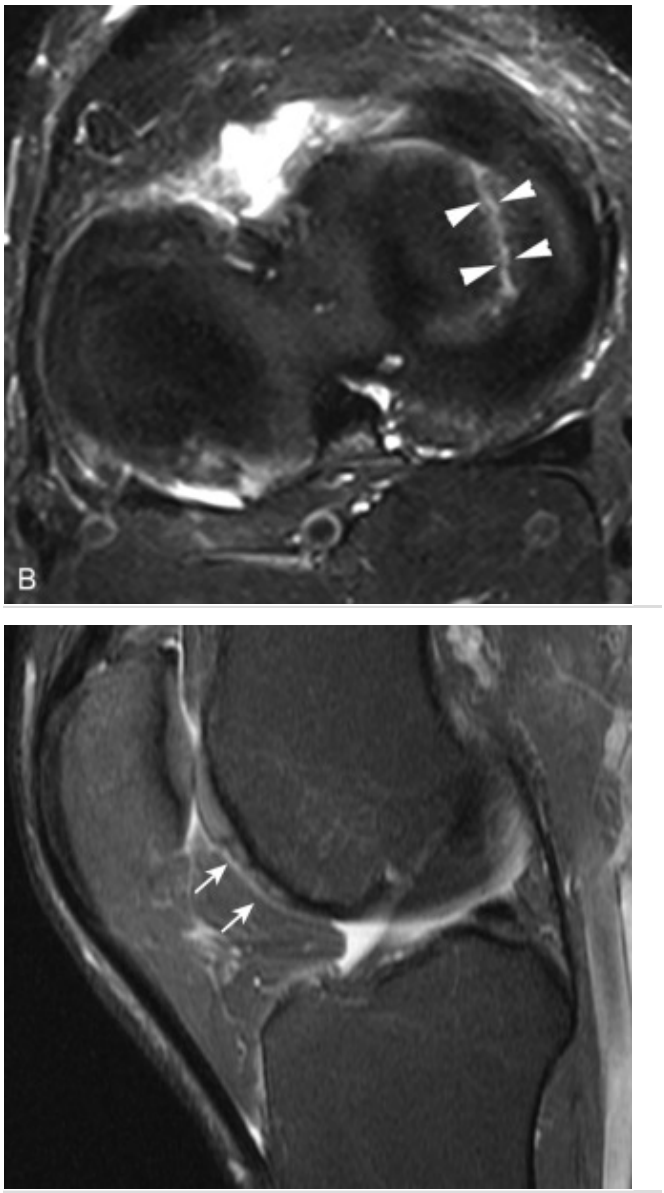


## Fig. 6.18

**Partial-width cartilage loss.** Sagittal T2W fat-suppressed image showing a partial-width cartilage abnormality within the trochlea ( *arrows* ).

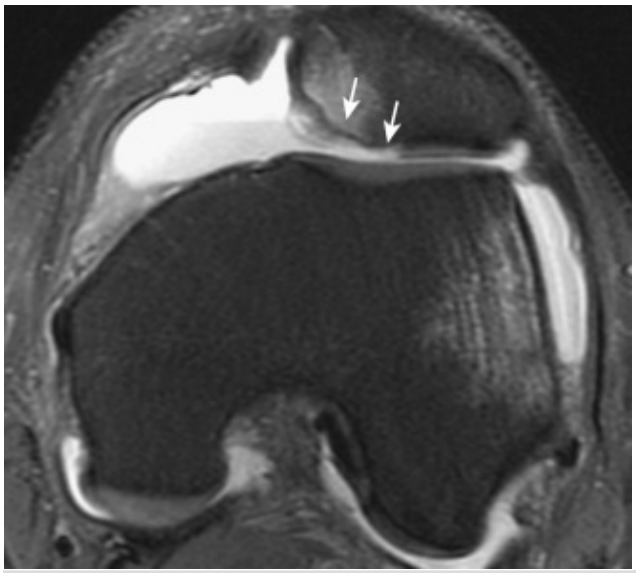

**Fig. 6.19**

**Full-thickness cartilage loss.** Axial T2W fat-suppressed image in a patient who had a patellar dislocation. Marked full-thickness cartilage loss at the apex of the patella ( *arrows* ). Recognizing cartilage loss in a patient with a patellar dislocation has treatment implications and is an important observation.

**Fig. 6.20**

**Full-thickness cartilage loss.** Sagittal proton density ( **A** ) and STIR ( **B** ) images show a full-thickness cartilage defect as evidenced by the fluid signal replacing the intermediate signal of the hyaline articular cartilage along the weight-bearing portion of the medial femoral condyle ( *arrowheads* ). **C,** Sagittal STIR image reveals multiple loose bodies in the lateral suprapatellar pouch ( *arrow* ).

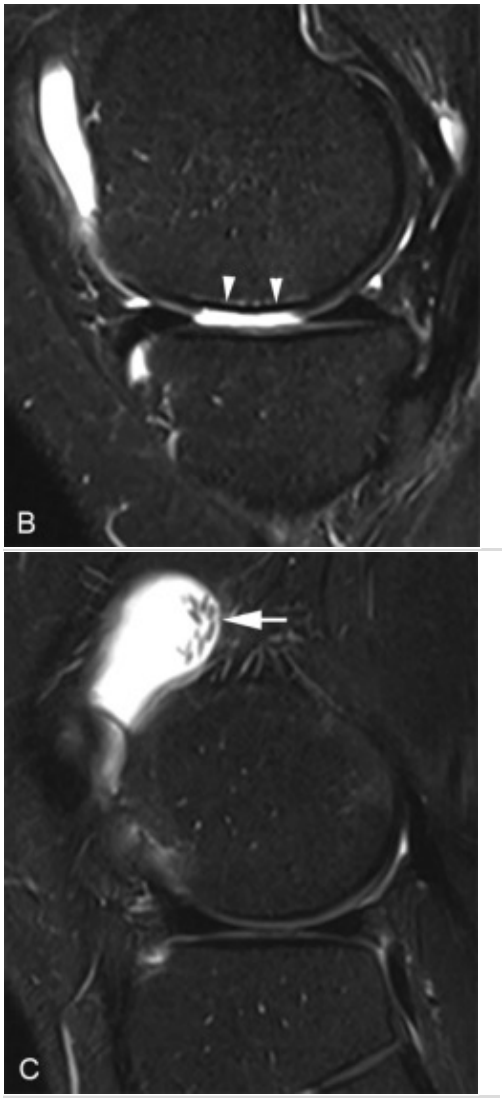


**Fig. 6.21**

**Delamination. A,** Sagittal STIR image displays an area of subchondral edema–like signal (contusion) as well as fluid signal at the cartilage–bone interface (tidemark) ( *arrowheads* ) in this patient after an acute injury. **B,** Sagittal STIR image in the same patient 2 weeks later after an episode of locking of the knee shows that the area of delaminated cartilage has become displaced, leaving a full-thickness defect at that site.

When evaluating articular cartilage, it is important to choose an appropriate MRI sequence. By selecting a sequence that has a TE between 30 and 60 msec (a combination of proton density and T2 weighting), this should allow for differentiation between cartilage, subchondral bone, and joint fluid. The addition of fat suppression is another option that is preferred by some; however, magnetic field inhomogeneities (such as those occuring with orthopedic hardware) can result in nonuniform fat suppression and wreak havoc with the images. In these cases, short tau inversion recovery (STIR) imaging should provide more homogeneous fat suppression and reliable cartilage evaluation.

Three dimensional (3D) volume-spoiled GRASS (gradient-recalled acquisition in the steady state) with fat suppression has been highly touted to increase the accuracy of articular cartilage evaluation in the knee. Although this sequence does provide elegant images of cartilage, it does not allow for assessing the subchondral bone; 3D fast spin echo imaging may provide good depiction of articular cartilage as well as other internal structures of the knee using a single acquisition, but has not yet replaced 2D imaging in routine clinical practice.

One difficulty in identifying cartilage abnormalities is simply looking at all the cartilage surfaces. We have found that it is preferable to have a cartilage-sensitive sequence in all three planes because the conspicuity of an abnormality often is prominent in one of the planes and very subtle in the other two. We probably spend as much time inspecting the knee for cartilage abnormalities as we do looking at the remainder of the knee.

Imaging at 3 T can provide better resolution, and perhaps increased confidence, but even at this field strength, it is still imperative to employ a proper sequence for cartilage evaluation.

## Summary

MRI has utility in imaging for arthritis particularly in the early stages of diagnosis and after treatment. Radiologists should be familiar with the MRI appearances of the most common arthritides. Cartilage imaging is considered an essential part of the imaging of any joint, and therefore, cartilage-sensitive sequences should be built into all joint protocols. A full description of each chondral abnormality should be made, rather than attempting to place it into one of many grading systems.

## Suggested Reading

## Arthritis

Ash Z., Marzo-Ortega H.: Ankylosing spondylitis—the changing role of imaging.Skeletal Radiol 2012; 41: pp. 1031-1034.

Bangert B., Modic M., Ross J., et. al.: Hyperintense disks on T1-weighted MR images: correlation with calcification.Radiology 1995; 195: pp. 437-444.

Brossmann J., Preidler K.W., Daenen B., et. al.: Imaging of osseous and cartilaginous intraarticular bodies in the knee—comparison of MR imaging and MR arthrography with CT and CT arthrography in cadavers.Radiology 1996; 200: pp. 509-517.

Emad Y., Ragab Y., El-Naggar A., et. al.: Gadolinium-enhanced MRI features of acute gouty arthritis on top of chronic gouty

involvement in different joints.Clin Rheumatol 2015; 34: pp. 1939-1947.

Flemming D.J., Hash T.W., Bernard S.A., et. al.: MR imaging assessment of arthritis of the knee.Magn Reson Imaging Clin N Am. 2014; 22: pp. 703-724.

Garner H.W., Bestic J.M.: Benign synovial tumors and proliferative processes.Semin Musculoskelet Radiol 2013; 17: pp. 177-178.

Girish G., Glazebrook K.N., Jacobsen J.A.: Advanced imaging in gout.AJR Am J Roentgenol 2013; 2015: pp. 515-525.

Hughes T.H., Sartoris D.J., Schweitzer M.E., et. al.: Pigmented villonodular synovitis: MRI characteristics.Skeletal Radiol 1995; 24: pp. 7-12.

Kiss E., Keusch G., Zanetti M., et. al.: Dialysis-related amyloidosis revisited.AJR Am J Roentgenol 2005; 185: pp. 1460-1467.

Kurer M., Baillod R., Madgwick J.: Musculoskeletal manifestations of amyloidosis.J Bone Joint Surg [Br] 1991; 73: pp. 271-276.

Levine D.S., Forbat S.M.: SaifuddinA. MRI of the axial skeletal manifestations of ankylosing spondylitis.Clin Radiol 2004; 59: pp. 400-413.

Major N., Helms C., Genant H.: Calcification demonstrated as high signal intensity on T1-weighted MR images of the disks of the lumbar spine.Radiology 1993; 189: pp. 494-496.

Naidich J.B., Mossey R.T., McHeffey A.B., et. al.: Spondyloarthropathy from long-term hemodialysis.Radiology 1988; 167: pp. 761-764.

Narvaez J.A., Narvaez J., De Lama E., et. al.: MR imaging of early rheumatoid arthritis.RadioGraphics 2010; 30: pp. 143-165.

## Cartilage

Abraham C.L., Bangerter N.K., McGavin L.S., et. al.: Accuracy of 3D dual echo steady state (DESS) MR arthrography to quantify acetabular cartilage thickness.J Magn Reson Imaging 2015; 42: pp. 1329-1338.

Crema M.D., Roemer F.W., Marra M.D., et. al.: Articular cartilage in the knee: current MR imaging techiques and application in clinical practice and research.RadioGraphics 2011; 31: pp. 37-62.

Disler D.G., McCauley T.R., Kelman C.G., et. al.: Fat-suppressed three-dimensional spoiled gradient-echo MR imaging of hyaline cartilage defects in the knee—comparison with standard MR imaging and arthroscopy.AJR Am J Roentgenol 1996; 167: pp. 127-132.

Gagliardi J.A., Chung E.M., Chandnani V.P., et. al.: Detection and staging of chondromalacia patellae: relative efficacies of conventional MR imaging, MR arthrography, and CT arthrography.AJR Am J Roentgenol 1994; 163: pp. 629-636.

Kendell S.D., Helms C.A., Rampton J.W., et. al.: MRI appearance of chondral delamination injuries of the knee.AJR Am J Roentgenol 2005; 184: pp. 1486-1489.

Kijowski R., Blankenbaker D.G.: Woods, et al. Clinical usefulness of adding 3D cartilage imaging sequences to a routine knee MR protocol.AJR Am J Roentgenol 2011; 196: pp. 159-167.

Recht M.P., Piraino D.W., Paletta G.A., et. al.: Accuracy of fat-suppressed three-dimensional spoiled gradient-echo flash MR imaging in the detection of patellofemoral articular cartilage abnormalities.Radiology 1996; 198: pp. 209-212.

Ronga M.: AngerettiG, FerraroS, et al. Imaging of articular cartilage: current concepts.Joints 2014; 2: pp. 137-140.

Zilkens C., Tiderius C.J., Krauspe R., et. al.: Current knowledge and importance of dGEMRIC techniques in diagnosis of hip joint diseases.Skeletal Radiol 2015; 44: pp. 1073-1083.

## References

Ash and Marzo-Ortega, 2012. Ash Z., and Marzo-Ortega H.: Ankylosing spondylitis—the changing role of imaging. Skeletal Radiol 2012; 41: pp. 1031-1034
Cross Ref (http://dx.doi.org/10.1007/s00256-012-1466-6)

Bangert et al., 1995. Bangert B., Modic M., Ross J., et al: Hyperintense disks on T1-weighted MR images: correlation with calcification. Radiology 1995; 195: pp. 437-444
Cross Ref (http://dx.doi.org/10.1148/radiology.195.2.7724763)

Brossmann et al., 1996. Brossmann J., Preidler K.W., Daenen B., et al: Imaging of osseous and cartilaginous intraarticular bodies in the knee—comparison of MR imaging and MR arthrography with CT and CT arthrography in cadavers. Radiology 1996; 200: pp. 509-517
Cross Ref (http://dx.doi.org/10.1148/radiology.200.2.8685349)

Emad et al., 2015. Emad Y., Ragab Y., El-Naggar A., et al: Gadolinium-enhanced MRI features of acute gouty arthritis on

top of chronic gouty involvement in different joints. Clin Rheumatol 2015; 34: pp. 1939-1947
Cross Ref (http://dx.doi.org/10.1007/s10067-015-2895-0)

Flemming et al., 2014. Flemming D.J., Hash T.W., Bernard S.A., et al: MR imaging assessment of arthritis of the knee. Magn Reson Imaging Clin N Am. 2014; 22: pp. 703-724
Cross Ref (http://dx.doi.org/10.1016/j.mric.2014.07.012)

Garner and Bestic, 2013. Garner H.W., and Bestic J.M.: Benign synovial tumors and proliferative processes. Semin Musculoskelet Radiol 2013; 17: pp. 177-178
Cross Ref (http://dx.doi.org/10.1055/s-0033-1343095)

Girish et al., 2013. Girish G., Glazebrook K.N., and Jacobsen J.A.: Advanced imaging in gout. AJR Am J Roentgenol 2013; 2015: pp. 515-525
Cross Ref (http://dx.doi.org/10.2214/AJR.13.10776)

Hughes et al., 1995. Hughes T.H., Sartoris D.J., Schweitzer M.E., et al: Pigmented villonodular synovitis: MRI characteristics. Skeletal Radiol 1995; 24: pp. 7-12

Kiss et al., 2005. Kiss E., Keusch G., Zanetti M., et al: Dialysis-related amyloidosis revisited. AJR Am J Roentgenol 2005; 185: pp. 1460-1467

Kurer et al., 1991. Kurer M., Baillod R., and Madgwick J.: Musculoskeletal manifestations of amyloidosis. J Bone Joint Surg [Br] 1991; 73: pp. 271-276
Cross Ref (http://dx.doi.org/10.1302/0301-620X.73B2.2005153)

Levine and Forbat, 2004. Levine D.S., and Forbat S.M.: SaifuddinA. MRI of the axial skeletal manifestations of ankylosing spondylitis. Clin Radiol 2004; 59: pp. 400-413
Cross Ref (http://dx.doi.org/10.1016/j.crad.2003.11.011)

Major et al., 1993. Major N., Helms C., and Genant H.: Calcification demonstrated as high signal intensity on T1-weighted MR images of the disks of the lumbar spine. Radiology 1993; 189: pp. 494-496
Cross Ref (http://dx.doi.org/10.1148/radiology.189.2.8210379)

Naidich et al., 1988. Naidich J.B., Mossey R.T., McHeffey A.B., et al: Spondyloarthropathy from long-term hemodialysis. Radiology 1988; 167: pp. 761-764
Cross Ref (http://dx.doi.org/10.1148/radiology.167.3.3363137)

Narvaez et al., 2010. Narvaez J.A., Narvaez J., De Lama E., et al: MR imaging of early rheumatoid arthritis. RadioGraphics 2010; 30: pp. 143-165

Abraham et al., 2015. Abraham C.L., Bangerter N.K., McGavin L.S., et al: Accuracy of 3D dual echo steady state (DESS) MR arthrography to quantify acetabular cartilage thickness. J Magn Reson Imaging 2015; 42: pp. 1329-1338
Cross Ref (http://dx.doi.org/10.1002/jmri.24902)

Crema et al., 2011. Crema M.D., Roemer F.W., Marra M.D., et al: Articular cartilage in the knee: current MR imaging techiques and application in clinical practice and research. RadioGraphics 2011; 31: pp. 37-62

Disler et al., 1996. Disler D.G., McCauley T.R., Kelman C.G., et al: Fat-suppressed three-dimensional spoiled gradient-echo MR imaging of hyaline cartilage defects in the knee—comparison with standard MR imaging and arthroscopy. AJR Am J Roentgenol 1996; 167: pp. 127-132
Cross Ref (http://dx.doi.org/10.2214/ajr.167.1.8659356)

Gagliardi et al., 1994. Gagliardi J.A., Chung E.M., Chandnani V.P., et al: Detection and staging of chondromalacia patellae: relative efficacies of conventional MR imaging, MR arthrography, and CT arthrography. AJR Am J Roentgenol 1994; 163: pp. 629-636
Cross Ref (http://dx.doi.org/10.2214/ajr.163.3.8079858)

Kendell et al., 2005. Kendell S.D., Helms C.A., Rampton J.W., et al: MRI appearance of chondral delamination injuries of the knee. AJR Am J Roentgenol 2005; 184: pp. 1486-1489
Cross Ref (http://dx.doi.org/10.2214/ajr.184.5.01841486)

Kijowski and Blankenbaker, 2011. Kijowski R., and Blankenbaker D.G.: Woods, et al. Clinical usefulness of adding 3D cartilage imaging sequences to a routine knee MR protocol. AJR Am J Roentgenol 2011; 196: pp. 159-167

Recht et al., 1996. Recht M.P., Piraino D.W., Paletta G.A., et al: Accuracy of fat-suppressed three-dimensional spoiled gradient-echo flash MR imaging in the detection of patellofemoral articular cartilage abnormalities. Radiology 1996; 198: pp. 209-212
Cross Ref (http://dx.doi.org/10.1148/radiology.198.1.8539380)

Ronga, 2014. Ronga M.: AngerettiG, FerraroS, et al. Imaging of articular cartilage: current concepts. Joints 2014; 2: pp. 137-140

Zilkens et al., 2015. Zilkens C., Tiderius C.J., Krauspe R., et al: Current knowledge and importance of dGEMRIC techniques in diagnosis of hip joint diseases. Skeletal Radiol 2015; 44: pp. 1073-1083
Cross Ref (http://dx.doi.org/10.1007/s00256-015-2135-3)